

## Counter-propagating streamers in an atmospheric-pressure helium plasma jet

This content has been downloaded from IOPscience. Please scroll down to see the full text.

2017 J. Phys. D: Appl. Phys. 50 205201

(<http://iopscience.iop.org/0022-3727/50/20/205201>)

View [the table of contents for this issue](#), or go to the [journal homepage](#) for more

Download details:

IP Address: 138.253.76.4

This content was downloaded on 27/04/2017 at 16:38

Please note that [terms and conditions apply](#).

You may also be interested in:

[Computational study of the afterglow in single and sequential pulsing of an atmospheric-pressure plasma jet](#)

M I Hasan and J W Bradley

[Computational study of the interaction of cold atmospheric helium plasma jets with surfaces](#)

Douglas Breden and Laxminarayan L Raja

[Computational model of the interaction of a helium atmospheric-pressure jet with a dielectric surface](#)

M I Hasan and J W Bradley

[The evolution of atmospheric-pressure low-temperature plasma jets: jet current measurements](#)

Erdinc Karakas, Mehmet Arda Akman and Mounir Laroussi

[Kinetics and dynamics of nanosecond streamer discharge in atmospheric-pressure gas bubble suspended in distilled water under saturated vapor pressure conditions](#)

Ashish Sharma, Dmitry Levko, Laxminarayan L Raja et al.

[Dynamics of a guided streamer \('plasma bullet'\) in a helium jet in air at atmospheric pressure](#)

J-P Boeuf, L L Yang and L C Pitchford

[Atmospheric-pressure plasma transfer across dielectric channels and tubes](#)

Zhongmin Xiong, Eric Robert, Vanessa Sarron et al.

[A Brief Study on the Ignition of the Non-Thermal Atmospheric Pressure Plasma Jet from a Double Dielectric Barrier Configured Plasma Pencil](#)

Asma Begum, Mounir Laroussi and M. R. Pervez

# Counter-propagating streamers in an atmospheric-pressure helium plasma jet

M I Hasan<sup>1,3</sup>, U Cvelbar<sup>2</sup>, J W Bradley<sup>3</sup> and J L Walsh<sup>1,3</sup>

<sup>1</sup> Centre for Plasma Microbiology, Department of Electrical Engineering and Electronics, The University of Liverpool, Brownlow Hill, L69 3GJ, United Kingdom

<sup>2</sup> Department of Surface Engineering and Electronics, Institute 'Jozef Stefan', Ljubljana, 1000, Slovenia

<sup>3</sup> Department of Electrical Engineering and Electronics, University of Liverpool, Brownlow Hill, L69 3GJ, United Kingdom

E-mail: [j.l.walsh@liv.ac.uk](mailto:j.l.walsh@liv.ac.uk)

Received 6 February 2017, revised 6 March 2017

Accepted for publication 30 March 2017

Published 21 April 2017



## Abstract

This study explores an atmospheric pressure plasma jet impinging on a downstream dielectric surface using a 2D numerical plasma fluid model. It is demonstrated that a counter-propagating discharge ignites at the exposed dielectric surface when the discharge is ignited using negative polarity voltage pulses with fall times in the microsecond range. Two distinct streamer discharges are created, a cathode-directed streamer propagating upstream toward the cathode, and an anode-directed streamer propagating parallel to the dielectric surface facing the gas flow. The surface discharge propagating parallel to the dielectric surface deposits negative surface charge. It is also shown that driving an APPJ with a negative applied potential significantly increases the  $O_2^-$  time-averaged flux to the dielectric surface while decreasing the  $O_2^+$  time-averaged flux.

Keywords: atmospheric-pressure, plasma jet, plasma model


(Some figures may appear in colour only in the online journal)

## 1. Introduction

In the last decade, atmospheric pressure plasma jets (APPJs) have attracted considerable attention due to their ability to generate a long and reactive plume of plasma species that extend several cm's beyond the jet's exit. Such characteristics mean APPJ systems are ideally suited for a wide variety of applications, including surface decontamination [1], materials processing [2], wound healing and dental hygiene [3, 4]. Given their application potential, APPJs have been the subject of intensive experimental and computational investigation. It is well established that the discharge produced by an APPJ is in the form of a train of fast propagating streamers (also known as plasma bullets, fast ionization wave, or pulsed atmospheric plasma streamers). These propagate in the noble gas channel at velocities much higher than that of the background

flow velocity [5, 6]. When a dielectric surface is placed downstream, the impinging plasma bullets deflect at the surface and propagate in a parallel direction to the dielectric surface, depositing positive surface charge [7, 8]. Under certain generation conditions, it has been shown that a plasma bullet can ignite at the dielectric surface and propagate in the opposite direction, toward the powered electrode [9–13]: this can be considered as the 'reverse' direction of propagation in the region outside the dielectric tube [11]. This phenomenon has mainly been observed in the presence of a dielectric surface downstream on the negative cycle of the applied voltage waveform.

In general, most computational studies have focused on the propagation of the discharge generated by a positive applied potential. Few studies have focused on plasma bullets produced by a negative applied potential, in spite of many experimental reports which show clear differences between the two types of operation in terms of structure, intensity and chemistry [14, 15]. Of the numerical studies focusing on negative pulsed operation of APPJs, Nadis studied the operation of a

 Original content from this work may be used under the terms of the [Creative Commons Attribution 3.0 licence](https://creativecommons.org/licenses/by/3.0/). Any further distribution of this work must maintain attribution to the author(s) and the title of the work, journal citation and DOI.

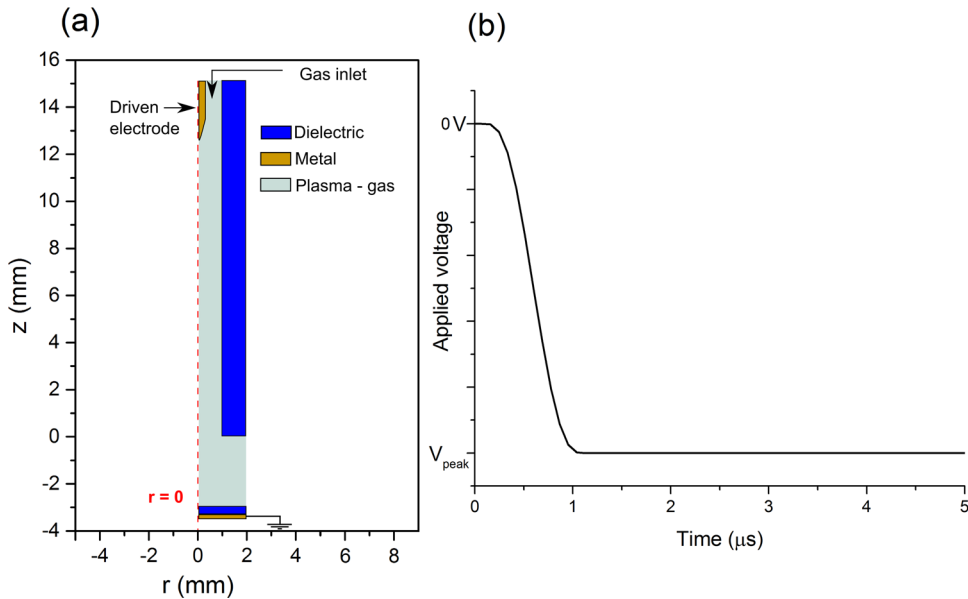


**Figure 1.** (a) The computational domain marking the dielectric and the gas region where plasma exists, (b) the time profile of the applied waveform assumed in the model (corresponding to a negative value of  $V_{\text{peak}}$ ).

negatively driven APPJ in open air [17] and Norberg *et al* considered the interaction between a negatively driven APPJ discharge and a partially conductive surface downstream of the jet [17–19]. In these reports, the discharge was operated under conditions where the generated plasma bullet was observed to propagate from the driven electrode to the dielectric surface.

In this work, a 2D axisymmetric fluid numerical model is used to study the characteristics of the counter-propagating bullet in a helium APPJ, driven by a negative applied potential. In essence, the discharge configuration simulated in this work is similar to that reported by Norberg *et al* [17–19]; however, the major difference is a considerably longer rise time of the applied potential, which is  $1 \mu\text{s}$  in this work compared to  $5 \text{ ns}$  in the work of Norberg *et al* [17–19]. Surprisingly, this longer rise time initiates a counter-propagating mode of operation, where the generated streamer propagates from the dielectric surface to the driving electrode. The model is also used to study the time-averaged fluxes of  $\text{O}_2^-$  and  $\text{O}_2^+$  associated with the counter-propagating discharge and provide a comparison with those produce in the conventional propagation direction.

## 2. Numerical model

The model used in this study is similar to our previous work described in Hasan *et al* [8], it is a 2D axisymmetric fluid model describing a helium jet impinging on a dielectric surface in ambient air conditions. Several minor modifications have been done to the model described in [8] for this work, including a reduction in the number of species considered: electrons,  $\text{He}^+$ ,  $\text{He}^*$  (helium excited to  $2^3 \text{ S}$  state),  $\text{He}_2^*$ ,  $\text{He}_2^+$ ,  $\text{N}_2^+$ ,  $\text{O}_2^+$ ,  $\text{O}_2^-$ , and their associated reactions. Moreover, a second modification was also made to the electrode geometry; which is depicted in figure 1(a) and comprised of an electrode needle 1 mm in length with an internal radius of curvature of  $10 \mu\text{m}$  at the tip. The downstream dielectric surface was situated 3 mm from the exit of the dielectric capillary. The

secondary electron emission coefficient of the pin electrode was set to 0.1 for all ions. The discharge was driven by the voltage profile shown in figure 1(b), which is a ramp function having a rise time of  $1 \mu\text{s}$ . The model was solved for a total of  $5 \mu\text{s}$  of discharge time. Three values of the applied potential were chosen:  $-4 \text{ kV}$ ,  $-6 \text{ kV}$ , and  $+6 \text{ kV}$  for comparison. For all cases considered, the rate of voltage change was adjusted to ensure the maximum voltage was reached at  $1 \mu\text{s}$ . Additionally, the feed gas flow rate was assumed to be 1.5 SLM with a negligible level of impurities. This gas feed is introduced in the domain through the boundary between the dielectric tube and the pin electrode as shown in figure 1(a). For the initial conditions, it was assumed that the plasma density in the vicinity of the pin electrode was  $10^{15} \text{ m}^{-3}$  which decayed exponentially over a distance of 3 mm to a value of  $10^{12} \text{ m}^{-3}$  everywhere else in the computational domain. This assumption accounts for the seed electrons and is motivated by the fact that the electric field is strong at the pin tip due to its curvature, even for low applied potentials. This implies that the electrons near the tip experience ohmic heating constantly, causing an increase in the local plasma density. This situation mimics what is observed in experiments where repetitive pulses are used and the discharge relies on seed electrons from previous pulses.

## 3. Results and discussion

This section will focus solely on the negative applied potentials, as positive applied potentials have been studied widely. Under negative potential excitation, a continuous plasma channel forms between the pin electrode and the dielectric surface downstream, the ignition and the expansion of this channel occurs through three phases. The first phase is a discharge driven by secondary-emitted electrons and ignited at the pin electrode, approximately  $0.3\text{--}0.6 \mu\text{s}$  from the simulation initiation. This discharge is followed by the ignition of two streamers,

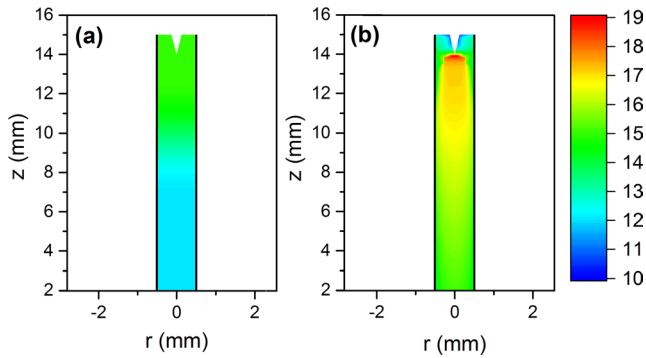


**Figure 2.** (a) Logarithm of electron density at  $0 \mu\text{s}$ , and (b) at  $2 \mu\text{s}$ . Both are shown for  $V_{\text{peak}} = -4\text{kV}$ . Panels (a) and (b) have the same legend. The domain is plotted only from  $z = 2\text{ mm}$  to  $16\text{ mm}$  to highlight the pin electrode.

the counter propagating streamer and the surface streamer (in a parallel direction along the downstream dielectric surface). These three distinct phases are discussed further in section 3.1, followed by a discussion on the time-averaged fluxes of  $\text{O}_2^-$  and  $\text{O}_2^+$  to the dielectric surface for the three investigated cases in section 3.2. For simplicity, the time-averaged fluxes will be referred to simply as fluxes in the remainder of this work.

### 3.1. Phase 1: pin electrode discharge

This discharge phase begins as soon as the applied potential begins to increase at the pin electrode (increase in absolute terms). The negative applied potential accelerates electrons in the initial plasma away from the pin electrode and accelerates ions toward it. The accelerated electrons aided by the secondary emitted electrons from the pin electrode start to ionize the gas around the pin electrode, causing the local plasma density to increase. This occurs at approximately  $0.5\text{--}0.6 \mu\text{s}$  from the beginning of the applied pulse in the  $-4\text{kV}$  case. Following this, the plasma spreads further into the dielectric tube driven by the strong axial electric field, extending beyond the region having a high initial plasma density, as figure 2 shows.

### 3.2. Phase 2: the counter-propagating streamer

The counter-propagating streamer starts to ignite at the dielectric surface approximately  $0.5 \mu\text{s}$  from the start of the applied voltage pulse, at a position close to the axis of symmetry. The electrons from the initial plasma are driven away from the negatively biased plasma and pushed toward the dielectric surface; depositing their charge and limiting the flow of other electrons to the same spatial position. This process directs the electron flux to another point on the dielectric surface that is further radially from the axis of symmetry. The directed electrons accelerated by the electric field gain enough energy to ionize the background gas, increasing the local plasma density near the dielectric surface and initiating streamer propagation. Given that the streamer is ignited at the surface of the dielectric, there are two possible paths for it to propagate; the first is in the upstream direction, creating the counter-propagating streamer. Alternatively, propagation can occur along the surface, creating the surface streamer

(discussed in the following section). The counter-propagating streamer moves from the dielectric surface toward the pin electrode. Since the pin electrode is negatively biased, the counter-propagating streamer is in the form of a cathode-directed streamer. While propagating outside of the dielectric tube (between the dielectric surface and the exit of the dielectric capillary), it follows a path along the radial mixing layer, which is defined as the transition zone between the helium jet and the surrounding ambient air. As the counter-propagating streamer approaches the exit of the tube, it can no longer propagate along the radial mixing layer. Instead, the propagation of the streamer head continues along the axis of symmetry, eventually entering the dielectric tube through its exit. As it enters the tube, the electric field in the streamer head and its propagation velocity increase noticeably. Figure 3 shows the axial electric field at various times as the counter-propagating streamer propagates inside the dielectric tube. The propagation in the dielectric tube continues until the streamer head reaches the diffusing plasma emanating from the pin electrode. At that point, the streamer structure is lost and a single glow-like discharge forms in the gap between the plasma surrounding the pin electrode and the plasma channel created by the counter-propagating streamer. The glow-like discharge can be seen by observing the uniformity of the electric field, by comparing figure 3(b), which shows the point before the transition, and figure 3(c) the point following the transition in to a glow-like discharge.

Under  $-6\text{kV}$  excitation the same process occurs, but at a faster rate. For instance, the streamer head enters the dielectric tube at approximately  $0.9 \mu\text{s}$  and propagates with an average velocity of  $70\text{ km s}^{-1}$  until it transitions into a glow-like discharge. Under  $-4\text{kV}$  excitation, the streamer head does not enter the dielectric tube until  $1.5 \mu\text{s}$ , and then propagates at  $15\text{ km} \cdot \text{s}^{-1}$ . Both of these velocities are similar to those reported for the downstream propagating streamers [5, 10], and are consistent with the experimental observations of the velocity of the counter-propagating streamer [11].

From a practical perspective, the ignition of a glow-like discharge in the dielectric tube could have a significant impact on the chemistry of the discharge in comparison with the conventional streamer discharge, particularly in cases where an admixture is added to the helium flow.

### 3.3. Phase 3: the surface discharge

The surface streamer ignites approximately  $0.1 \mu\text{s}$  after the counter-propagating streamer is created as described in section 3.2. Both the surface streamer and the counter-propagating streamer are ignited from the same point on the dielectric surface. The counter-propagating streamer creates a plasma channel extending from the dielectric surface to the streamer head. This plasma channel is located slightly off the axis of symmetry. As the plasma channel is held at a negative potential compared to its surroundings, the electrons experience a radial electric field that increases their energy enabling them to ionize the background gas. Some electrons are deposited on to the dielectric surface as they move parallel to it due to diffusion, charging the surface negatively at that spatial location.

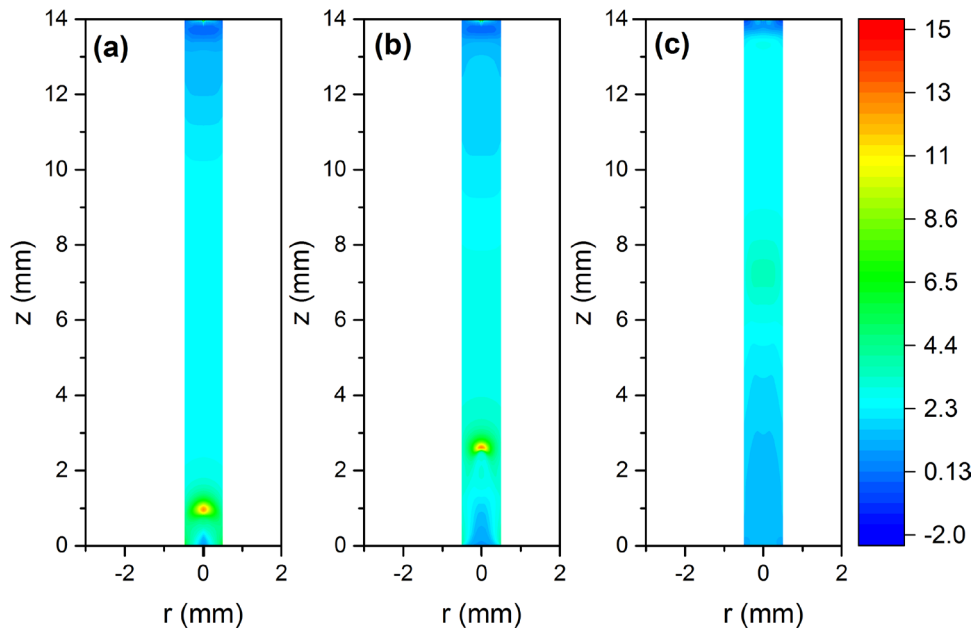


**Figure 3.** The axial electric field of the upstream discharge at (a)  $2 \mu\text{s}$ , (b)  $2.25 \mu\text{s}$ , and (c)  $2.5 \mu\text{s}$ . All taken for  $V_{\text{peak}} = -4\text{kV}$ . All the panels have the same legend. The legend is shown in units of  $\text{kV} \cdot \text{cm}^{-1}$ .

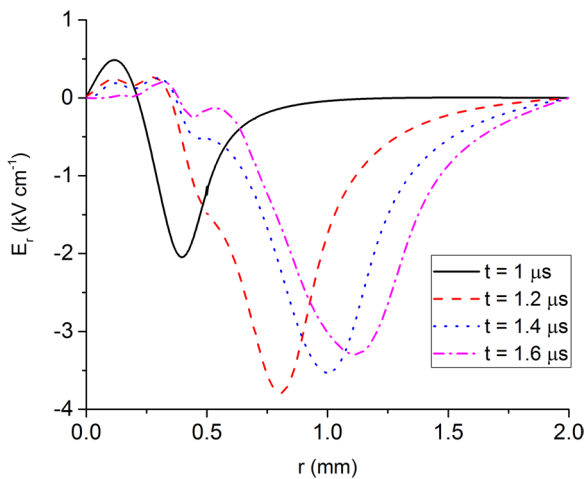


**Figure 4.** The radial electric field at the dielectric surface during the propagation of the surface streamer for  $V_{\text{peak}} = -4\text{kV}$ .

The deposited surface charge causes the maximum radial electric field to shift slightly in the radial outward direction where there is no surface charge covering the dielectric surface and the ground electrode under the dielectric surface is still ‘visible’ to the electrons. This shifted electric field, presented in figure 4, initiates a new cycle of ionization and surface charge deposition, resulting in a further shift in the field. It is through this mechanism that the surface streamer propagates. By the end of the simulation, the total surface charge deposited on the dielectric surface is negative for the negative applied potential cases compared to a positive surface charge for the 6kV case, as seen in figure 5.

The association of a counter-propagating streamer with negative surface charge was reported experimentally by Wild *et al* [13]. The peak electric field in the surface streamer is on the order of  $4\text{kV} \cdot \text{cm}^{-1}$  as shown in figure 4. This is noticeably less than the  $12\text{kV} \cdot \text{cm}^{-1}$  observed in the counter-propagating

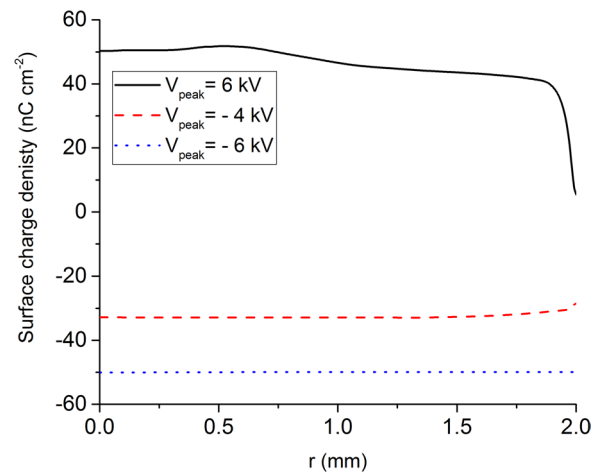


**Figure 5.** Surface charge density at the dielectric surface at  $5 \mu\text{s}$  for different applied potentials.

streamer, indicating that the surface streamer is significantly weaker in comparison.

Since the surface streamer is essentially propagating toward the ground electrode from the negatively biased plasma channel, it can be classified as an anode directed streamer, which has significantly different characteristics to those of a surface discharge seen when using a positive applied potential, which has characteristics akin to a cathode directed streamer [8]. The main difference lies in the electric field. With a negative applied potential, the radial electric field is weaker (peak of  $4\text{--}6\text{kV} \cdot \text{cm}^{-1}$ ) and is spread over a wider area compared to its counterpart in the positive applied potential case, where the electric field is relatively strong (peak of  $\sim 40\text{kV} \cdot \text{cm}^{-1}$ ) and is highly localized in the streamer head. These differences in the electric field between positively induced and negatively induced streamers were examined in [16].

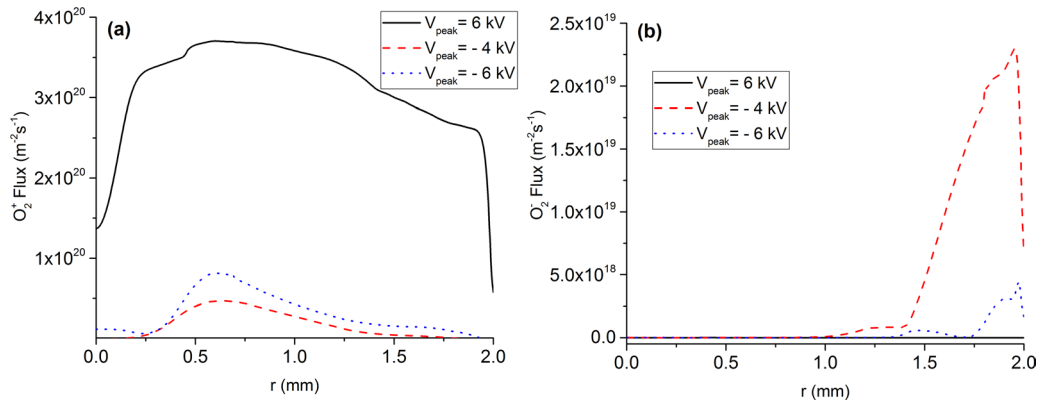


**Figure 6.** (a)  $\text{O}_2^+$  flux to the dielectric surface at  $5 \mu\text{s}$  for three applied voltages, (b)  $\text{O}_2^-$  flux to the dielectric surface at  $5 \mu\text{s}$  for three applied voltages.

The propagation mechanism described here for the surface streamer holds true for both cases of  $-4$  kV and  $-6$  kV. The only difference is that the surface streamer starts earlier for the  $-6$  kV and ignites at a stronger electric field with a maximum of at  $6 \text{ kV} \cdot \text{cm}^{-1}$  compared to that of  $-4$  kV.

### 3.4. Ionic oxygen fluxes to the dielectric surface

In this section, the fluxes of  $\text{O}_2^-$  and  $\text{O}_2^+$  to the dielectric surface under positive and negative excitation are compared as these are of considerable practical importance. Figure 6 shows the flux of  $\text{O}_2^-$  and  $\text{O}_2^+$  under  $-6$ ,  $-4$  and  $+6$  kV excitation.

It is clear from figure 6 that the flux of  $\text{O}_2^+$  peaks at a higher value than that of  $\text{O}_2^-$  for all the cases investigated in this work. This can be attributed to the fact that more  $\text{O}_2^+$  ions are generated in the discharge than  $\text{O}_2^-$  ions. The difference between the fluxes of  $\text{O}_2^+$  and  $\text{O}_2^-$  is the largest for  $V_{\text{peak}} = 6$  kV as a result of the strong axial electric field directed toward the surface. The high field increases the  $\text{O}_2^+$  flux and decreases the  $\text{O}_2^-$  flux to the surface. In the negative applied potential cases, the flux of negatively charged species (electrons and  $\text{O}_2^-$  ions) arrives at the surface while the surface streamer is propagating parallel to it, as explained in section 3.2. The flux of negatively charged species is dominated by the electrons everywhere on the surface. The  $\text{O}_2^-$  flux increases in the radial direction as a result of the increasing air fraction, which means more  $\text{O}_2^-$  ions are created and deposited on the surface. The  $\text{O}_2^+$  flux in the negative applied potential case peaks approximately  $0.7$  mm from the axis of symmetry, where an overlap between the counter-propagating streamer and the surface streamer occurs. The  $\text{O}_2^+$  flux also peaks at that position as a result of the attraction between  $\text{O}_2^+$  ions from the plasma channel created by counter-propagating streamer and the negative surface charge on the dielectric surface.

As detailed in section 3.3, the surface streamer is driven by a weaker electric field in the  $V_{\text{peak}} = -4$  kV case compared to  $V_{\text{peak}} = -6$  kV case. Consequently, the corresponding electron temperature in the  $V_{\text{peak}} = -4$  kV case is lower than that in  $V_{\text{peak}} = -6$  kV, which leads to more  $\text{O}_2^-$  ions being generated in the former case. As a result, the  $\text{O}_2^-$  flux to the surface is higher for the  $V_{\text{peak}} = -4$  kV case as indicated by figure 6.

## 4. Conclusions

To unravel the mechanisms behind the counter-propagating streamer propagation a pin electrode based helium atmospheric-pressure plasma jet (APPJ) was studied using a 2D plasma fluid model. The influence of negative and positive applied potentials to the pin electrode was considered. By driving the discharge with a rise time on the order of a  $\mu\text{s}$  causes the discharge to operate in a counter-propagation mode for negative applied potentials. In this mode, the discharge evolves through three distinct phases. In the first stage the discharge forms around the pin-electrode, where electrons are repelled by the negative potential and ignite a local discharge sustained by the secondary emitted electrons. The second phase of the discharge involves the generation of a counter-propagating streamer, where a cathode-directed streamer is ignited at the dielectric surface and propagates into the dielectric tube. Eventually the counter-propagating streamer turns into a glow-like discharge in the gap between the pin electrode and dielectric surface. Finally, in the third phase of the discharge the surface streamer is formed, which ignites shortly after the counter-propagating streamer. This is an anode direct discharge that propagates as a result of negative surface charge deposition on the dielectric surface.

The influence of a negative applied potential on the ionic fluxes to the dielectric surface is also considered. It was observed that the  $\text{O}_2^-$  flux to the dielectric surface is significantly increased when the discharge is driven by a negative applied potential, while the  $\text{O}_2^+$  flux decreases slightly. The increase in the  $\text{O}_2^-$  flux to the surface occurs due to the propagation mechanism of the surface streamer, where negatively charged species are attracted to the grounded electrode under the dielectric surface in areas where the surface charge density is low. The increase in the  $\text{O}_2^-$  flux is more noticeable in the  $-4$  kV case compared to  $-6$  kV case, as a result of the electric field driving the surface streamer being weaker in the former case, which corresponds to lower electron temperature and higher attachment rate of the electrons to  $\text{O}_2$ .

The results of this study indicate that there may be a possibility of controlling the time-averaged fluxes of  $\text{O}_2^-$  and  $\text{O}_2^+$  (and positively/negatively charged species in general) by changing the driving polarity of the discharge. Comparing this study to other studies with similar jet configurations, it also indicates that the rise time can be used to operate the

discharge in conventional mode or counter-propagating mode for the same polarity of the applied potential. From an application perspective, the ability to control the nature of charged species flux to a downstream surface is extremely important and such techniques could be employed in both materials processing and biomedical applications.

### Acknowledgments

The authors are grateful for UK Engineering and Physical Sciences Research Council (Project EP/N021347/1) and Innovate UK (Project 50769-377232) for providing support for this work. UC and JW acknowledge also support from NATO grant SPS.984555.

### References

- [1] Nishime T M C, Borges A C, Koga-Ito C Y, Machida M, Hein L R O and Kostov K G 2016 *Surf. Coat. Technol.* **312** 19
- [2] Oh J S and Bradley J W 2013 *Plasma Process. Polym.* **10** 839
- [3] Schmidt A, Bekeschus S, Wende K, Vollmar B and von Woedtke T 2017 *Exp Dermatol.* **26** 156
- [4] Claiborne D, McCombs G, Lemaster M, Akman M A and Laroussi M 2014 *Int. J. Dent. Hygiene* **12** 108
- [5] Teschke M, Kedzierski J, Finantu-Dinu E G, Korzec D and Engemann J 2005 *IEEE Trans. Plasma Sci.* **33** 310
- [6] Whalley R D and Walsh J L 2016 *Sci. Rep.* **6** 31756
- [7] Breden D and Raja L L 2014 *Plasma Sources Sci. Technol.* **23** 065020
- [8] Hasan M I and Bradley J W 2015 *J. Phys. D: Appl. Phys.* **48** 435201
- [9] Ito T, Raddenzati A, Shams A and Hamaguchi S 2010 *Japan. J. Appl. Phys.* **49** 100209
- [10] Nastuta A V, Topala I and Popa G 2011 *IEEE Trans. Plasma Sci.* **39** 2310
- [11] Gerling T, Nastuta A V, Bussiahn R, Kindel E and Weltmann K-D 2012 *Plasma Sources Sci. Technol.* **21** 034012
- [12] Sobota A, Guaitella O and Garcia-Caurel E 2013 *J. Phys. D: Appl. Phys.* **46** 372001
- [13] Wild R, Gerling T, Bussiahn R, Weltmann K-D and Stollenwerk L 2014 *J. Phys. D: Appl. Phys.* **47** 042001
- [14] Shi J, Zhong F, Zhang J, Liu D W and Kong M G 2008 *Phys. Plasmas* **15** 013504
- [15] Yonemori S and Ono R 2015 *Biointerphases* **10** 029514
- [16] Naidis G V 2011 *Appl. Phys. Lett.* **98** 141501
- [17] Norberg S A, Tian W, Johnsen E and Kushner M J 2014 *J. Phys. D: Appl. Phys.* **47** 475203
- [18] Norberg S A, Johnsen E and Kushner M J 2015 *J. Appl. Phys.* **118** 013301
- [19] Norberg S A, Johnsen E and Kushner M J 2016 *J. Phys. D: Appl. Phys.* **49** 185201